

Stamping Vital Cells—a Force-Based Ligand Receptor Assay

Uta Wienken and Hermann E. Gaub*

Chair of Experimental Physics & Center for NanoScience, Ludwig-Maximilians-University München, Munich, Germany

ABSTRACT Gaining information about receptor profiles on cells, and subsequently finding the most efficient ligands for these signaling receptors, remain challenging tasks in stem cell and cancer research as well as drug development. We introduce a live-cell method with great potential in both screening for surface receptors and analysing binding forces of different ligands. The technique is based on the molecular force assay, a parallel-format, high-throughput experiment on a single-molecule level. On human red blood cells, we demonstrate the detection of the interaction of N-acetyl- α -D-galactosaminyl residues with the lectin *helix pomatia* agglutinine and of the CD47 receptor with its antibody. The measurements are performed under nearly physiological conditions and still provide a highly specific binding signal. Moreover, with a detailed comparative force analysis on two cell types with different morphology, we show that our method even allows the determination of a DNA force equivalent for the interaction of the CD47 receptor and its antibody.

INTRODUCTION

Surface receptors and their interactions are a major focus of biomedical and pharmaceutical research due to their fundamental role in both signal transduction (1) and cell adhesion (2–4) as well as their involvement in cancer development and progression (5). In addition to the biochemical aspects of cell regulation and signaling, mechanical aspects play an important role (6–15) and must be considered. Still, the analysis of the binding behavior of such proteins remains challenging (16). In recent years, biochip technologies have steadily gained importance not only as a research tool for detecting protein-protein interactions in general, but also as a diagnostic device. The possibility of screening for a vast number of specific marker proteins in parallel lead to many different protein biochip formats (17,18).

Although fast and cost-saving, the principle of microarrays is unfortunately afflicted with certain restrictions. To probe protein-protein interactions in a highly parallel format, proteins have to be immobilized on a surface. Such nonphysiological conditions hold the possibility of denaturation of the protein. Considering the influence of conformational changes on protein-protein interactions, this method might easily lead to wrong results, such as unspecific binding of nontarget molecules or nonbinding of the natural target (18). An assay with membrane proteins seems even more problematic, because their hydrophobic transmembrane region makes it nearly impossible to immobilize such proteins on a surface. Consequently, they can only be probed if it is possible to do protein expression with the extracellular or intracellular domain or analyze single domains (19).

In this article we introduce what we believe to be a new live-cell assay, based on the molecular force assay (MFA) established by Albrecht et al. (20). So far, the MFA was

only applied to probe molecules immobilized on glass surfaces. The application of the MFA on cells offers the possibility of screening for receptors on the cell membrane with high throughput. Furthermore, it even allows access to the binding properties of such receptors under nearly physiological conditions.

MATERIALS AND METHODS

Production of elastomer stamps and chemical treatment

The stamps consisting of the silicone elastomer Sylgard (Dow Corning, Midland, MI) are fabricated as described by Xia et al. (21). They are 1 mm high and 1 mm in diameter with a square microstructure of $100 \times 100 \mu\text{m}^2$ and 5 μm in height. The pads' centers have a distance of 141 μm from each other. Before chemical modification, the stamps are ultrasonically cleaned in 50% aqueous isopropanol solution for 10 min, irradiated for another 10 min in an UV cleaner, activated in 12.5 % HCl overnight, and rinsed afterwards. Subsequently, the stamps are incubated for 30 min in 3-glycidoxypropyl-trimethoxysilane (ABCRC, Karlsruhe, Germany) to generate epoxide groups on the surface. After rinsing excess silane with isopropanol and ddH₂O, the stamps are stored in argon atmosphere at 6°C until usage. For DNA functionalization, the stamp is incubated in a borate buffered solution of amino-modified DNA in a saturated salt atmosphere overnight resulting in a covalent bond between stamp surface and DNA. For further treatment, the stamp is rinsed with water, passivated with a 4% bovine serum albumin (Carl Roth, Karlsruhe, Germany) solution for 10 min, and finally rinsed with water and dried with N₂.

Molecules

For all experiments, an amino-modified 45-bp DNA strand was coupled via the amino-epoxy reaction to the elastomer surface. A 5 \times hexaethyleneglycol spacer followed by a polyT spacer (10 \times thymine) prevents interactions of the DNA with the surface. The reference DNA complexes are generated by binding complementary DNA strands of different length to the amino-modified strand. The strands of varying length consist of 8, 9, 11, 13, 15, 30, and 45 nucleotides of complementary sequence followed by a Cy5 fluorescence dye and a biotin modification separated by a polyT spacer (20 \times thymine). For a minimum force measurement, a 20-nucleotide

Submitted August 22, 2013, and accepted for publication October 16, 2013.

*Correspondence: gaub@physik.uni-muenchen.de

Editor: Daniel Muller.

© 2013 by the Biophysical Society
0006-3495/13/12/2687/8 \$2.00



zipper-like DNA was used. In experiments with 15–45 bp the GC content of DNA is 60%, for shorter duplexes it is in a range between 62 and 67%. All DNA strands are purchased from IBA (Göttingen, Germany). The CD47 antibody (Klon CC2C5; BioLegend, San Diego, CA) and the lectin *helix pomatia* agglutinin (HPA; Sigma Aldrich, St. Louis, MO) were covalently linked to streptavidin using Lightning-Link streptavidin (Innova Biosciences, Cambridge, UK).

Modification of the stamp surface

Different solutions of complementary biotin-modified DNA strands with a Cy5 fluorescence dye marker and streptavidin-modified antibodies are mixed in a 1:1 stoichiometry in 1× phosphate-buffered saline (PBS) solution with 30 mM trehalose and are deposited with the microarray plotter (GIX I Microplotter; SonoPlot, Middleton, WI) on the microstructure of the stamp. After 5 min, the stamp is washed in 1× PBS, 1× PBS with 0.1% TWEEN, and again 1× PBS for 1 min each and then blocked with 4% bovine serum albumin for 10 min. Finally, the stamp is rinsed and kept in 1× PBS until usage. The measurements are conducted with solutions of 0.56 μM streptavidin-modified CD47 antibody and 0.56 μM streptavidin-modified HPA, which are combined with biotin-modified DNA strands of different length (zip, 8, 9, 11, 13, 15, 30, and 45 basepairs).

Cell culture

Human red blood cells (RBCs) are taken freshly from the finger pad of healthy volunteers, washed with 1× PBS, and centrifuged five times to separate the cells from the blood plasma. RBCs in 1× PBS suspension are then seeded on a poly-L-lysine (Biochrom, Berlin, Germany) -covered glass coverslip and incubated for 30 min at 37°C. RBCs are afterwards rinsed three times with 1× PBS to remove nonadherent cells. Measurements are performed in 1× PBS.

The human melanoma cell line M21 is provided by D. L. Morton (University of California, Los Angeles, CA) and is cultured in RPMI 1640 medium (GIBCO, Life Technologies, Paisley, UK) supplemented with 10% fetal bovine serum and 5 mM glutamine at 37°C in 5% CO₂ atmosphere. At least 24 h before experiments, cells are harvested with 0.01% EDTA and seeded on a glass coverslip. Directly before measurements, the culture medium is removed, and cells are rinsed three times with 1× PBS. The measurements are performed in CO₂-independent L-15 Leibovitz medium without phenol red (GIBCO, Life Technologies).

Experimental setup

The MFA measurements are conducted with a modified inverse epifluorescence microscope (Axio Observer Z1; Zeiss, Oberkochen, Germany). For the alignment of the elastomer stamp and cells, the probe stage can be positioned in the *x-y* direction. The elastomer stamp is adhered to a 12-mm diameter glass coverslip, and is attached at the glass block of the stamping unit by an elastomer-connecting piece.

The cell surface is approached by a high-precision stepper motor (Physik Instrumente, Karlsruhe, Germany) and then brought into close proximity by a piezo actuator (Piezosystem, Jena, Germany). The parallel alignment of the stamp to the cell surface is done by micrometer screws (OWIS, Staufen, Germany) and monitored by reflection interference contrast microscopy. Illumination is performed using high-power light-emitting diodes (627 nm peak wavelength, Thorlabs, Dachau, Germany) for fluorescence imaging and using a mercury arc lamp (Osram, Munich, Germany) for interference contrast microscopy.

Fluorescence analysis

Fluorescence pictures of the cells are recorded with an Andor iXon camera (Andor Technology, Belfast, UK) and analyzed with a self-written

LABVIEW software routine (National Instruments, München, Germany). For analysis, fluorescence pictures with 10× magnification displaying the complete stamping pattern are recorded. The data we gain is fluorescence intensity, which is proportional to the incoming light intensity. To account for the heterogeneity of the illumination profile, the pictures are corrected with a picture of the illumination. The background intensity is measured in the nonfluorescent area between the pads. Several background measurements are averaged and then subtracted. For the analysis of the fluorescent areas, a grid is overlaid and aligned in the pictures of the stamp and of the cells after stamping. According to the grid, the mean intensity of the areas is measured, and afterwards, the mean intensity of the fluorescent areas on the cells is divided by the mean intensity of the corresponding pads on the stamp. In this way, we gain the relative fluorescence transfer on the cells. Hence, a relative fluorescence transfer of 0.05 means that 5% of the ligands on the stamp are transferred to the cells.

RESULTS AND DISCUSSION

Experimental approach

The MFA allows an analysis of binding forces of receptor-ligand interactions on a single molecule level by performing ensemble measurements. A molecular reference complex with known binding force is compared to the binding force of a probe complex. Both complexes are clamped in series between two surfaces. When separated, the molecular complex with the weaker bond is more likely to rupture, and a fluorescent label indicates the outcome of the experiment (20,22). In conventional MFA experiments, reference and probe consist of DNA or RNA duplexes. The typical setup (23) offers the possibility to analyze, e.g., the effect of a single basepair mismatch or nucleic-acid binding molecules (20–27). The setup for the *in vitro* analysis of membrane proteins with the MFA differs in some aspects. Most importantly, one surface is exchanged for a layer of living cells exposing certain receptors. These cell surface receptors and their possible ligands serve as probe, while the reference still consists of DNA. The DNA reference complex is immobilized on an elastomer surface. The specific ligand for a cell surface receptor is linked to the reference complex via a biotin-avidin chemistry (Fig. 1 A).

When contacting the cells with the elastomer stamp, reference and probe are clamped in series between rubber and cell surface. Like in standard MFA experiments, the molecular complex with the weaker bond is more likely to rupture upon separating the surfaces, and a fluorescent label at the reference complex indicates the outcome of the experiment. These single-molecule measurements are now performed in a highly parallel format by functionalizing the elastomer stamp with such molecular balances. However, in contrast to conventional MFA experiments, the number of force balances on the elastomer surface is much higher than the number of receptors at the cell surface. Consequently, with this setup there are many more incomplete than complete force balances, and thus, the ratio of the fluorescence intensity of the two surfaces provides no information about the strength of binding forces. The only

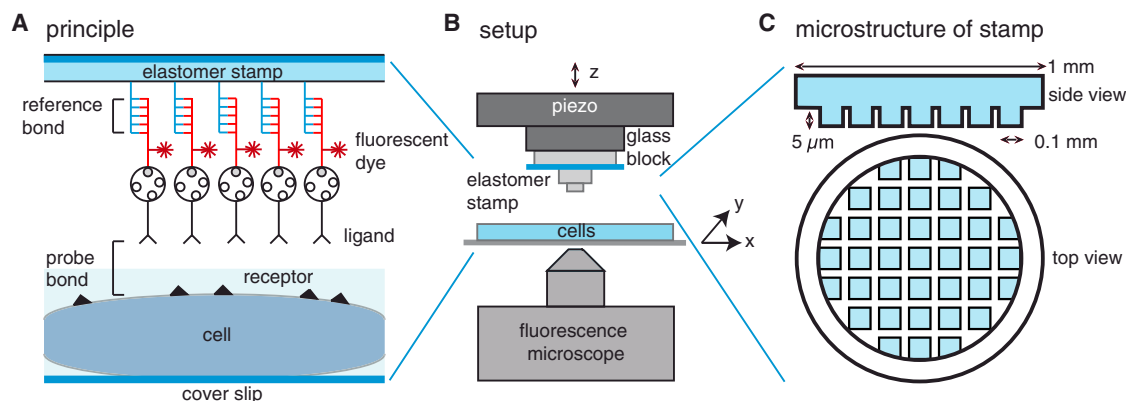


FIGURE 1 Experimental setup. (A) The principle of force balances in this experiment is illustrated. A reference bond and the probe bond are clamped in series between two surfaces; one is an elastomer stamp and the other is a cell's surface that exposes the receptor to analyze. The elastomer stamp is functionalized with the reference bond that consists of a DNA duplex with biotin, to which the probe molecule is linked via streptavidin. Both surfaces are brought into close contact and then are retracted. The weaker of the two bonds is more likely to rupture. A fluorescent dye at the reference complex displays the outcome of the experiment. (B) The experiment is monitored with an epi-fluorescence microscope with an x - y stage and an additional glass block to which the functionalized elastomer stamp is adhered. The glass block can be accurately adjusted in z position with a piezo, and its tilt can be leveled out with micrometer screws to ensure that both surfaces are parallel. (C) A scheme of the microstructure of the elastomer stamp is shown. The stamp is 1 mm in diameter with elevated pads of $100 \times 100 \mu\text{m}^2$. To see this figure in color, go online.

parameter relevant for this experiment is the fluorescence transfer onto the cells.

A scheme of the experimental setup is shown in Fig. 1 B. Before conducting the experiment, the stamp is prepared with DNA force balances of various strengths. Each pad can be functionalized with different force balances by a microplotter. To abate suction and turbulence during the retraction of the stamp, the elastomer stamp has a microstructure with elevated pads of $100 \times 100 \mu\text{m}^2$ (shown in Fig. 1 C). During the experiment, the cell surface is approached by a high-precision stepper motor and then brought into close proximity by a piezo actuator. Because the exact parallel alignment of the elastomer surface and the cells is crucial to ensure an all-over contact for the whole elastomer surface with the cells during the experiment, the tilt of the glass block can be adjusted with micrometer screws. The parallel alignment is controlled by interference contrast microscopy allowing for adjustments in the nanometer range.

After the cells have been in contact with the functionalized stamp for 1 min, the stamp is retracted with a velocity of 50 nm/s. The precise definition of the retraction speed is controlled using the piezo actuator. After separation, fluorescence images of the stamped cells are taken. Fig. 2 A shows a typical $10\times$ magnification fluorescence image, which is then used for detailed analysis of a complete experiment. The fluorescence picture with $40\times$ magnification gives a more detailed view of single blood cells (Fig. 2 B). They are only labeled in areas where the functionalized pads of the stamp were in contact.

Screening assay

The experiment described in the following shows that the application of the MFA on cells is a valuable method to

screen for multiple cell surface receptors in parallel. This is of great interest for medical research and drug development, because the lack or overexpression of surface receptors is often linked to diseases (28,29). We demonstrate the high specificity of detection for this method with two different ligands. The first ligand is an antibody against the CD47 receptor. The CD47 receptor is a transmembrane protein found on nearly every human cell in an appropriate density (30). The second ligand is the lectin HPA (31) that binds to n -acetyl- α -D-galactosaminyl residues (galNAc), a special glycolipid rest in the glycocalyx of human red blood cells (RBCs). This glycolipid rest is exposed in a high density on RBCs of only blood group A. On RBCs of blood group O or B, galNAc is absent (32). Grandbois et al. (33) previously analyzed this receptor-ligand complex with AFM. They obtained rupture forces of ~ 35 pN for a single bond rupture of the galNAc-HPA complex at a retraction velocity of $6 \mu\text{m/s}$. According to Strunz et al. (34), this corresponds to a DNA duplex shorter than 10 bp. Because the rupture force of the DNA duplex is given by a rupture

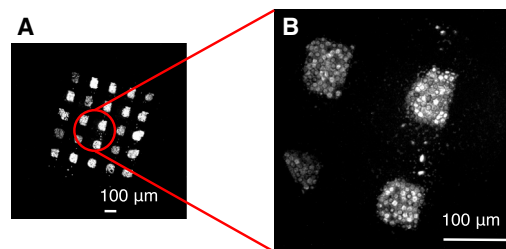


FIGURE 2 Fluorescence pictures of RBCs after contact. (A) The picture with $10\times$ magnification depicts the fluorescence pattern of the pads. (B) At $40\times$ magnification, single fluorescently labeled blood cells are visible. To see this figure in color, go online.

force distribution with nonzero width, it is possible to obtain a specific fluorescence transfer in a force range around the distribution's mean value. Given the unknown rupture force of the CD47 receptor and its antibody, a DNA reference force higher than 10 bp was chosen to cover a broad range of possible interaction strengths. With the used 15-bp DNA reference complex, additionally, the nonspecific fluorescence transfer could be reduced. HPA was deposited with a microplotter on every second pad in a chessboardlike pattern, and the CD47 antibody was transferred to the remaining pads (Fig. 3, A and B).

The first pad is always excluded from the measurements, because it is the starting and end point for the plotting process. Here, different solutions might accidentally mix up. With only one stamp, two different experiments are conducted: the first is on the RBCs of blood group A, and the second is on the RBCs of blood group O. This is possible because the number of receptors on the cells is much lower than the number of ligands on the stamp.

In the first experiment, the RBCs of blood group A precisely exhibit the pattern on the microstructure of the

elastomer as a fluorescence transfer pattern (Fig. 3 C), indicating that both galNAc and the CD47 receptor are exposed on the cells. The fluorescence transfer for HPA is higher than for CD47 antibody. One explanation could be a higher galNAc density on the cell surface. A higher binding force of galNAc to HPA, on the other hand, would lead to the same result, because the DNA duplex is more likely to rupture. Repeating the experiment with the same stamp on RBCs of blood group O, we only obtained the chessboardlike pattern of the CD47 antibody (Fig. 3 D). Clearly, we gained no fluorescence transfer for the lectin HPA on blood group O. This directly shows the absence of galNAc on blood group O. Furthermore, these results strongly suggest the elimination of unspecific interactions with this method, because the force to open the 15-bp DNA strand exceeds the strength of possible unspecific interactions. Similar experiments with a 9-bp DNA strand confirm the results. These experiments demonstrate that the MFA on living cells in combination with the microplotter technique is a powerful tool for the parallel screening for cell surface receptors.

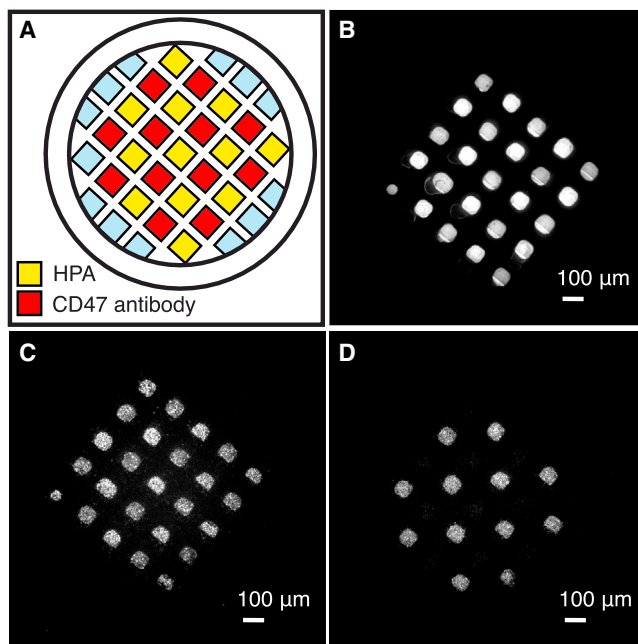


FIGURE 3 Detection of CD47 receptor and galNAc on human RBCs. (A) Force balances, consisting of a 15-bp DNA duplex as reference force and the CD47 antibody or the lectin HPA, respectively, are deposited in a chessboardlike pattern. (B) The fluorescence picture shows the elastomer stamp after functionalization. With one stamp, two different experiments are conducted. (C) Postcontact fluorescence picture demonstrates that we obtain a fluorescence signal for both the CD47 receptor and galNAc on cells of blood group A with slightly different intensities. This difference might be due to different ligand densities on the cells or a lower binding force of the receptor-ligand complex. (D) In the fluorescence image of the cells of blood group O after contact, no fluorescence transfer is observed for the pads functionalized with the lectin. This is due to the absence of galNAc in blood group O and clearly demonstrates the reduction of unspecific interactions with this method. To see this figure in color, go online.

Force measurements on RBCs

Because the MFA is primarily a method for highly sensitive force measurements (20), using the MFA on cells to reveal binding characteristics of the receptor-ligand bond seems a logical direction. The comparison of binding forces of different ligands provides valuable information about the interaction parameters, and hence, is of high interest for basic research and drug development. By performing a comparative force measurement, we circumvent elaborate direct force measurements like AFM experiments. Instead, we compare the binding force of the receptor-ligand complex of interest to a reference molecule that in case of the DNA is easier to analyze than the receptor-ligand complex (34). DNA is very well suited for those comparative force measurements, because the rupture force between duplexes may be programmed in a wide range by choosing attachment geometry, overlap length, and sequence (34,35).

In a single experiment, the pads of the elastomer stamp are functionalized with different DNA lengths linked to the ligand. The ligand binds to the receptor upon contact with the cell surface, and upon retraction, the reference or the probe bond ruptures in a stochastic process. The shorter the DNA duplex, the weaker the reference bond, and the more readily it breaks, resulting in a fluorescence transfer to the cell surface. Dependent on the length of the DNA duplexes and on the according strength of the reference bonds, we expect to obtain three regimes. For high reference forces corresponding to long DNA duplexes, we expect a minimum fluorescence transfer. On the other hand, for short DNA duplexes with a low reference force, we should obtain saturation of fluorescence transfer. In between these two regimes we expect a gradient, and specifically, the case

that the probability of bond rupture is 50% (i.e., when the reference force equals the force of the probe bond).

We conducted detailed force analyses with the CD47 antibody and the HPA on RBCs. For the analysis of the CD47 receptor, we functionalized an elastomer stamp with force balances consisting of the CD47 antibody and eight different lengths of DNA double strands (zip, 8, 9, 11, 13, 15, 30, and 45 bp) corresponding to different reference forces (Fig. 4 A).

For a maximum transfer, we use a 20-bp DNA, called “zip DNA”, that opens one basepair after the other. This offers the advantage that it is a thermodynamically stable strand that mirrors the rupture force of a single basepair. Zip DNA, therefore, defines the maximum fluorescence transfer. The geometry of the remaining duplexes is designed in a way that the force affects both 5'-ends of the double strand, resulting in a shear force. The fluorescence image of the RBCs after the contact process (Fig. 4 B) already reveals that pads with short DNA duplexes (corresponding to low reference forces) lead to more fluorescence transfer onto cells than pads with long DNA as a reference force. The graph obtained by explicit data analysis of three similar measurements (Fig. 4 C)

shows the maximum fluorescence transfer for the zip DNA and the short 8- and 9-bp DNA duplexes. This indicates that the binding force of antibody and receptor exceeds the reference force in this regime. A further increase in the number of basepairs corresponding to higher reference forces leads to a rapid change in fluorescence intensity. For long strands (30 and 45 bp), the fluorescence intensity hardly decreases, indicating that the binding force of the DNA duplex is higher than the force of antibody and receptor. A fit with a Boltzmann sigmoidal function displays a force equivalent of 10.5 ± 0.32 bp DNA duplex for the CD47 antibody and its receptor. Having a closer look at the data points, the sigmoidal fit represents only an approximation for our data. For the long DNA strands, we still observe a decrease in fluorescence transfer with increasing DNA length, even if the DNA length exceeds the DNA force equivalent of the interaction. This can be explained by the nonzero width of the rupture force distribution of the DNA reference. Thus, we also obtain a specific transfer for long DNA strands with interaction strengths stronger than the force equivalent. In contrast to this, in the screening assay (Fig. 3), the cells lack the necessary receptor for a specific transfer. Hence, the experiment

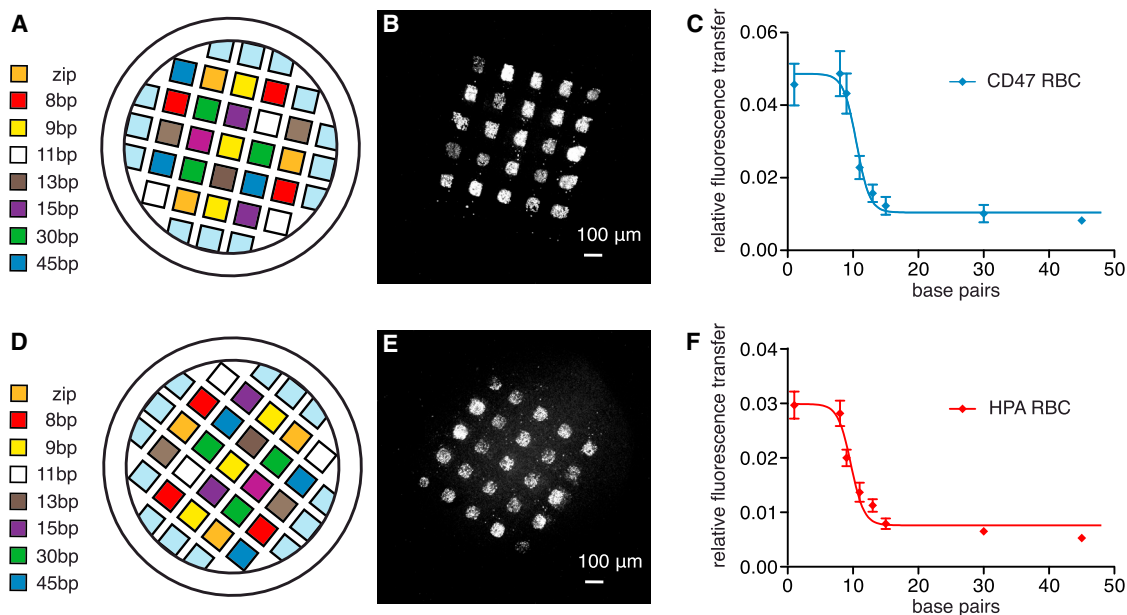


FIGURE 4 Detailed force measurements on RBCs for CD47 antibody and HPA. (A) A stamp is functionalized with force balances consisting of the CD47 antibody and DNA duplexes of eight different lengths varying from 8 to 45 bp that correspond to different reference forces increasing with DNA length. The maximum fluorescence transfer is defined by a 20-bp DNA strand that opens basepair by basepair like a zipper and is named “zip DNA”. It is thermodynamically stable and mirrors the binding force of a single DNA basepair. (B) The fluorescence picture of the cells after contact already depicts higher fluorescence intensities for lower reference forces. (C) The mean fluorescence transfer of three measurements is shown in the graph. For low reference forces (8- and 9-bp duplexes), we obtain the maximum transfer defined by the zip DNA. With increasing DNA length, which represents an increasing reference force, we observe a rapid decrease in fluorescence intensity. When further increasing the DNA length to 45 bp, the intensity stays nearly constant. A Boltzmann sigmoidal fit displays a 50% value of 10.5 ± 0.32 bp DNA. (D) For a force analysis of the HPA-galNAc complex, the lectin was deposited on an elastomer stamp together with eight different DNA lengths. (E) The fluorescence picture of the cells after contact similarly shows higher intensities for pads with short DNA duplexes and very low intensities for long DNA. (F) The mean fluorescence transfer of four measurements displays a maximum transfer only for duplexes of 8 bp. An increase in DNA length corresponds to higher reference forces and leads to a transition. For high reference forces exerted by 30- and 45-bp DNA duplexes, the change in intensity is minimal. The 50% value of the Boltzmann sigmoidal fit is 9.7 ± 0.46 bp DNA. To see this figure in color, go online.

without the according receptor yields only unspecific fluorescence transfer, which is significantly below the specific transfer.

In a similar experiment, a second receptor-ligand complex, consisting of the glycolipid rest galNAc and its ligand HPA, was analyzed. Because the affinity of the HPA for galNAc is only in the 10^{-4} M regime (33), a shift to lower forces is expected. For the rupture forces analysis, balances with HPA and again eight different DNA lengths (zip, 8, 9, 11, 13, 15, 30, and 45 bp) are bound onto different pads of the elastomer stamp (Fig. 4 D). The fluorescence transfer onto the cells is depicted in Fig. 4 E. Again, pads with short DNA duplexes lead to high intensities on the cells, whereas pads with long DNA duplexes transfer little fluorescence to the cells. A detailed data analysis of four different measurements (Fig. 4 F) shows that the maximum fluorescence transfer is only obtained with the zip and 8-bp duplex DNA. Increasing the reference force leads to a transition towards lower fluorescence transfer. Longer duplexes (15, 30, and 45 bp) produce a minimum in fluorescence transfer. A Boltzmann sigmoidal fit yields a force equivalent of 9.7 ± 0.46 bp DNA for the HPA bound to galNAc. Compared to the force analysis of the CD47 antibody and its receptor, we obtain the expected shift to lower forces for the low-affinity ligand HPA. Grandbois et al. (33) obtained rupture forces for the galNAc-HPA complex of ~ 35 pN at a retraction velocity of $6 \mu\text{m/s}$. Considering the data that Strunz et al. (34) gained from AFM measurements with DNA duplexes, a most probable rupture force of 35 pN at this retraction velocity would be due to a DNA duplex shorter than 10 bp. Thus, compared to literature, the force equivalent for HPA is a reasonable value.

Force analyses on M21 cells

We demonstrate in the following that the force analysis with the MFA can be applied on different types of living cells with differing morphology and is not restricted to RBCs; we also conducted force analyses with the CD47 antibody on M21 melanoma cells. Again, we functionalized the stamp with the same DNA duplexes (Fig. 5 A).

The picture of the fluorescence transfer on the cells exhibits brighter regions for the zip DNA and short DNA duplexes (Fig. 5 B). Explicit data analysis of two measurements reveals two states and a gradient (Fig. 5 C). For the force equivalent for the CD47 receptor and its antibody on M21 cells, the Boltzmann fit yields a value of 9.8 ± 0.81 bp DNA. Comparing this to the force equivalent for the CD47 receptor on RBCs, a slightly lower value is found for the M21 melanoma cells. This shift might be generated by variations in the receptor expression that influences the affinity in different cells. Additionally, the signal/noise ratio decreases compared to the measurements on RBCs. This might be due to variations in the cell height and a less uniform distribution on the coverslip. Moreover, a lower

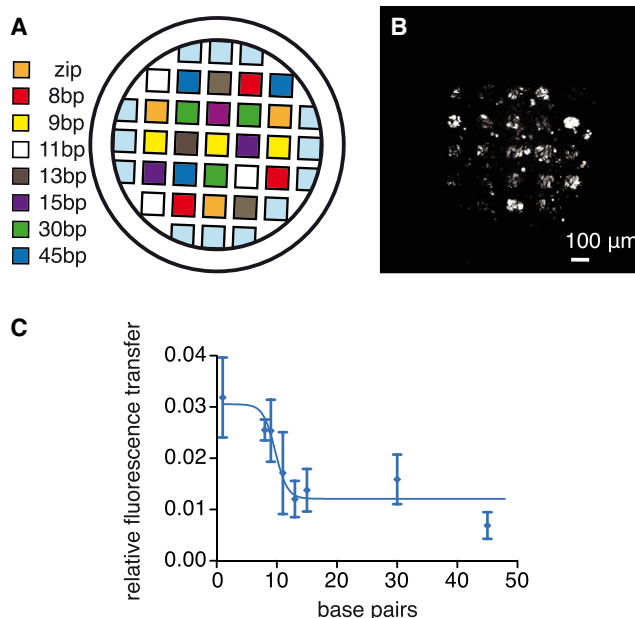


FIGURE 5 Force analysis of the CD47 receptor on M21 melanoma cells. (A) The elastomer stamp is functionalized with the CD47 antibody and DNA duplexes of eight different lengths as reference. (B) The fluorescence picture of the cells after contact clearly depicts the maximum fluorescence transfer defined by the zip DNA, and the transfer for 8-bp duplexes is notably higher than for longer reference duplexes. (C) The graph shows mean fluorescence transfer of two measurements. Again, two states can be distinguished: a maximum and a minimum fluorescence transfer. For the transition, the Boltzmann sigmoidal fit yields a 50% value of 9.8 ± 0.81 bp DNA. Compared to the analysis of the CD47 receptor on RBCs, the binding force for this receptor on M21 cells is shifted to a shorter DNA duplex that corresponds to a lower binding force. To see this figure in color, go online.

fluorescence transfer is observed for the M21 cells, which might be caused by a lower receptor density on these cells. However, the obtained signal/noise ratio allows for a reliable force analysis conducted directly on living cells.

See the [Supporting Material](#) for additional discussions.

CONCLUSION

Considering the highly important role of membrane proteins in physiological and pathological processes, and thus, their potential for medical and pharmaceutical research, there is a great demand for methods for the *in vitro* analysis of cell surface receptors. However, the research on membrane proteins remains challenging, and methods for their investigation are rare. One method to deal with transmembrane proteins is to stain living or fixed cells with specific fluorescently labeled ligands and analyze them by flow cytometry. For the staining process, cells are incubated with the ligand for a certain time and then washed to get rid of the excess ligand (36). Still, there is the possibility that in the absence of the target the ligand binds unspecifically and with lower affinity to another molecule on the cell surface, thereby

leading to a false-positive result. By using stains with different emission wavelengths, it is possible to detect a few different types of surface molecules at the same time, yet this method does not yield any information about the binding properties of the receptor under investigation. Employing AFM, the mechanical properties of receptor-ligand complexes on cells can be analyzed in detail, and rupture forces can be measured very accurately on a single molecule level (37–41). However, this technique is very time-consuming, and thereby not suitable for a high-throughput screening for membrane receptors on cells.

In this article we demonstrated that the MFA applied on living cells is a powerful method to do parallel screenings for cell surface receptors at nearly physiological conditions. At the same time, by delivering the ligand to the cell surface against a certain reference force, the method excludes unspecific interactions that might lead to biased results. The possibility to do a parallel screening for receptors on living cells without unspecific interactions makes this application attractive for healthcare and drug design. Moreover, we proved that it is possible to determine a DNA force equivalent for the receptor of interest by the variation of DNA reference forces. We have shown that the force equivalent for the low-affinity binder HPA is lower than for the CD47 antibody on RBCs. Additionally, we determined the force equivalent for the CD47 receptor on M21 melanoma cells and demonstrated that our method can be applied on living cells of cultured cell lines. Altogether, by the analysis of binding forces, our method provides access to the force threshold that is, e.g., necessary for a specific delivery of molecules on vital cells. Moreover, we gain highly valuable information about binding characteristics of receptors that help finding and evaluating possible ligands in cancer research and drug design. In summary, these qualities make the MFA on cells a powerful, effective, and widely applicable tool for health care, research, and drug development.

SUPPORTING MATERIAL

Discussion of Unspecific Fluorescence Transfer, Discussion of the Influence of Contact Force and Contact Time, and one figure are available at [http://www.biophysj.org/biophysj/supplemental/S0006-3495\(13\)01144-2](http://www.biophysj.org/biophysj/supplemental/S0006-3495(13)01144-2).

The authors thank Katja Limmer, Daniela Aschenbrenner, Marcus Otten, Dr. Philip Severin, and Dr. Martin Benoit for helpful discussions and Katherine Erlich for suggestions on the manuscript. Furthermore, we thank Dr. Diana Pippig and Katja Limmer for being healthy volunteers for the RBC experiments.

The authors thank the European Research Council and the Deutsche Forschungsgemeinschaft for support.

REFERENCES

- Smok, R. G., and L. M. Gierasch. 2009. Sending signals dynamically. *Science*. 324:198–203.
- Cavallaro, U., and G. Christofori. 2004. Cell adhesion and signaling by cadherins and Ig-CAMs in cancer. *Nat. Rev. Cancer*. 4:118–132.
- Parsons, J. T., A. R. Horwitz, and M. A. Schwartz. 2010. Cell adhesion: integrating cytoskeletal dynamics and cellular tension. *Nat. Rev. Mol. Cell Biol.* 11:633–643.
- Papuseva, E., and C.-P. Heisenberg. 2010. Spatial organization of adhesion: force-dependent regulation and function in tissue morphogenesis. *EMBO J.* 29:2753–2768.
- Simpson, R. J., and D. S. Dorow. 2001. Cancer proteomics: from signaling networks to tumor markers. *Trends Biotechnol.* 19:40–48.
- Puchner, E. M., and H. E. Gaub. 2012. Single-molecule mechanoenzymatics. *Annu. Rev. Biophys.* 4:497–518.
- Evans, E. A., and D. A. Calderwood. 2007. Forces and bond dynamics in cell adhesion. *Science*. 316:1148–1153.
- Vogel, V., and M. P. Sheetz. 2009. Cell fate regulation by coupling mechanical cycles to biochemical signaling pathways. *Curr. Opin. Cell Biol.* 21:38–46.
- Schwartz, M. A., and D. W. DeSimone. 2008. Cell adhesion receptors in mechanotransduction. *Curr. Opin. Cell Biol.* 20:1–6.
- Katz, B. Z., E. Zamir, ..., B. Geiger. 2000. Physical state of the extracellular matrix regulates the structure and molecular composition of cell-matrix adhesions. *Mol. Biol. Cell.* 11:1047–1060.
- Janmey, P. A., and C. A. McCulloch. 2007. Cell responses to mechanical stimuli. *Annu. Rev. Biomed. Eng.* 9:1–34.
- Bershadsky, A., M. Kozlov, and B. Geiger. 2006. Adhesion-mediated mechanosensitivity: a time to experiment and a time to theorize. *Curr. Opin. Cell Biol.* 18:472–481.
- Alenghat, F. J., and D. E. Ingber. 2002. Mechanotransduction: all signals point to cytoskeleton, matrix, and integrins. *Sci. STKE*. 119:1–4.
- Puchner, E. M., and H. E. Gaub. 2010. Exploring the conformation-regulated function of titin kinase by mechanical pump and probe experiments with single molecules. *Angew. Chem. Int. Ed.* 49:1147–1150.
- Puchner, E. M., A. Alexandrovich, ..., M. Gautel. 2008. Mechanoenzymatics of titin kinase. *Proc. Natl. Acad. Sci. USA*. 105:13385–13390.
- Zhu, H., and M. Snyder. 2001. Protein arrays and microarrays. *Curr. Opin. Chem. Biol.* 5:40–45.
- Chen, H., C. Jiang, ..., J. Kong. 2009. Protein chips and nanomaterials for application in tumor marker immunoassays. *Biosens. Bioelectron.* 24:3399–3411.
- Zhu, H., and M. Snyder. 2003. Protein chip technology. *Curr. Opin. Chem. Biol.* 7:55–63.
- Cunningham, F., and C. M. Deber. 2006. Optimizing synthesis and expression of transmembrane peptides and proteins. *Methods*. 41:370–380.
- Albrecht, C., K. Blank, ..., H. E. Gaub. 2003. DNA: a programmable force sensor. *Science*. 301:367–370.
- Xia, Y., and G. M. Whitesides. 1998. Soft lithography. *Annu. Rev. Mater. Sci.* 28:153–184.
- Albrecht, C. H., H. Clausen-Schaumann, and H. E. Gaub. 2006. Differential analysis of biomolecular rupture forces. *J. Phys. Condens. Matter*. 18:581–599.
- Severin, P. M. D., D. Ho, and H. E. Gaub. 2011. A high throughput molecular force assay for protein-DNA interactions. *Lab chip*. 11:856–862.
- Ho, D., K. Falter, ..., H. E. Gaub. 2009. DNA as a force sensor in an aptamer-based biochip for ATP. *Anal. Chem.* 81:3159–3164.
- Limmer, K., D. Aschenbrenner, and H. E. Gaub. 2013. Sequence-specific inhibition of Dicer measured with a force-based microarray for RNA ligands. *Nucleic Acids Res.* 41:e69.
- Severin, P. M. D., and H. E. Gaub. 2012. DNA-protein binding force chip. *Small*. 8:3269–3273.

27. Dose, C., D. Ho, ..., C. H. Albrecht. 2007. Recognition of "mirror-image" DNA by small molecules. *Angew. Chem. Int. Ed.* 46:8384–8387.
28. Oldenborg, P. A., Z. Zheleznyak, ..., F. P. Lindberg. 2000. Role of CD47 as a marker of Self on red blood cells. *Science*. 288:2051–2054.
29. Petitclerc, E., S. Strömblad, ..., P. C. Brooks. 1999. Integrin α V β 3 promotes M21 melanoma growth in human skin by regulating tumor cell survival. *Cancer Res.* 59:2724–2730.
30. Brown, E. J., and W. A. Frazier. 2001. Integrin-associated protein (CD47) and its ligands. *Trends Cell Biol.* 11:130–135.
31. Sanchez, J.-F., J. Lescar, ..., E. P. Mitchell. 2006. Biochemical and structural analysis of *helix pomatia* agglutinin. *J. Biol. Chem.* 281:20171–20180.
32. Torres, B. V., and D. F. Smith. 1988. Purification of Forssman and human blood group A glycolipids by affinity chromatography on immobilized *helix pomatia* lectin. *Anal. Biochem.* 170:209–219.
33. Grandbois, M., W. Dettmann, ..., H. E. Gaub. 2000. Affinity imaging of red blood cells using an atomic force microscope. *J. Histochem. Chemochem.* 48:719–724.
34. Strunz, T., K. Oroszlan, ..., H.-J. Güntherodt. 1999. Dynamic force spectroscopy of single DNA molecules. *Proc. Natl. Acad. Sci. USA.* 96:11277–11282.
35. Wang, X., and T. Ha. 2013. Defining single molecular forces required to activate integrin and Notch signaling. *Science*. 340:991–994.
36. Bendall, S. C., E. F. Simonds, ..., G. P. Nolan. 2011. Single-cell mass cytometry of differential immune and drug responses across a human hematopoietic continuum. *Science*. 332:687–696.
37. Helenius, J., C.-P. Heisenberg, ..., D. J. Müller. 2008. Single-cell force spectroscopy. *J. Cell Sci.* 121:1785–1791.
38. Medalsy, I., U. Hensen, and D. J. Müller. 2011. Quantifying chemical and physical properties of native membrane proteins at molecular resolution by force-volume AFM. *Angew. Chem. Int. Edit.* 50:12103–12108.
39. Dufrene, Y. F., and D. J. Müller. 2001. Force nanoscopy of living cells. *Curr. Biol.* 21:212–216.
40. Friedrichs, J., J. Helenius, and D. J. Müller. 2010. Quantifying cellular adhesion to extracellular matrix components by single-cell force spectroscopy. *Nat. Protoc.* 10:1353–1361.
41. Schmitz, J., and K. E. Gottschalk. 2008. Mechanical regulation of cell adhesion. *Soft Matter*. 4:1373–1387.